Progress In Electromagnetics Research C, Vol. 24, 161–171, 2011

SHORT-RANGE UWB WIRELESS LINK IN WPAN SCENARIOS

A. Vorobyov[1, 2, *] and A. Yarovoy[2]

[1]Institut d'Electronique et de Télécommunications de Rennes, UMR CNRS 6164, Université de Rennes 1, 35042 Rennes Cedex, France

[2]Delft University of Technology, International Research Center for Telecom and Radar (IRCTR), Mekelweg 4, 2628 CD Delft, The Netherlands

Abstract—We investigate experimentally and theoretically Ultra-Wideband (UWB) wireless transmission in different WPAN scenarios. Short-range UWB wireless link (wireless fire-wire) have been studied theoretically and experimentally. Different mutual positions and distances between the antennas have been investigated. It was found that the reactive antenna coupling might decrease power budget as much as 15 dB by an antenna separation of 5 mm.

1. INTRODUCTION

UWB communication systems have recently received increasing attention from the wireless community; they are characterized by a wide signal spectrum and low radiated power spectral density. One of the most interesting realizations of UWB radio systems is the impulse radio [1] which might be used in multiple applications, one of them being wireless body area network [2]. UWB communication systems for personal/body wireless area network can't be successfully implemented without achieving an understanding of phenomena related to near-field properties of antennas, their near-field coupling and impact of a human body in direct vicinity of antennas on the wireless link.

Majority of previous studies of transmission in WPAN scenarios (such as those described in [3–5]) did not take into account the frequency dependency (thus actually ignore UWB nature of wireless link) and focused mainly on the typical LOS and NLOS channels. Others like [6] and [7] considered this frequency dependency, but

Received 11 August 2011, Accepted 26 September 2011, Scheduled 27 September 2011

* Corresponding author: Alexander V. Vorobyov (alexander.vorobyov@gmail.com).

did not take into consideration possible human body influence during indoor, outdoor or on-body UWB channel measurements [15, 16].

Some of papers (e.g., [2]) showed that the human body has an impact on UWB antenna performances and, consequently, system design. Regarding mutual coupling of closely placed antennas (which might happen in on-body wireless as well as in wireless fire-wire application), near-field effects and reactive coupling between antennas might result in considerable deviations of the link power budget from Friis equation. For instance in paper [14] author have presented a new modulation technique, called pulse harmonic modulation, that suits wideband, low power data transmission across inductive telemetry links, particularly in the implantable medical devices applications.

In this paper we perform a thorough investigation of UWB wireless transmission on short ranges focusing on near-field phenomena. In our studies we use electrically small antennas of electric type as the most appropriate antenna class for this application. Where possible, both theoretical and experimental studies are done. We perform a systematic study on antenna near-field and near-field wireless transmission. We investigate the electrical field strength in the vicinity of a single antenna and transmission through a near-field-coupled antenna pair (typical for fire-wire and on-body communication scenarios). Different mutual positions and distances between the antennas will be taken into consideration. Theoretical results are verified experimentally.

The paper is organized as follows: Section 2 describes the Impulse Radio measurement setup, Section 3 focuses on transmission through a near-field wireless channel. Conclusions are given in Section 4.

2. IMPULSE RADIO SETUP

The UWB IR measurement setup is illustrated in Figure 1, and includes such blocks as sampling unit, digital sampling converter ZX10400, generator K263-2, computer with preset software, 20 dB attenuator, receive and transmit antennas. For connection between units we used "Sucoflex" cables to avoid high attenuation.

In all experiments we have used in-house developed elliptically-shaped dipole antenna with balanced feeding [8, 9]. This antenna is capable of radiating a 200 ps monocycle pulse. (Figure 2). This particular antenna was optimized to operate in a frequency band 1 GHz to 5 GHz. The antenna radiation patterns and antenna gain given in Figures 2(b), (c).

The pulse generator is connected to the transmit antenna via a 2 meter RF cable and a 20 dB attenuator. The antenna is connected

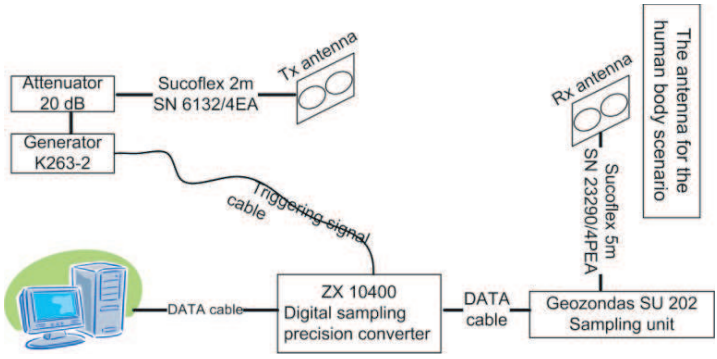

Figure 1. UWB Impulse Radio measurement setup.

(a)

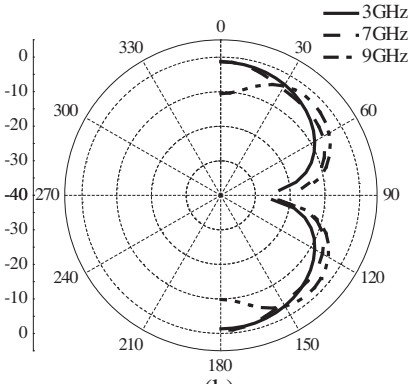

(b)

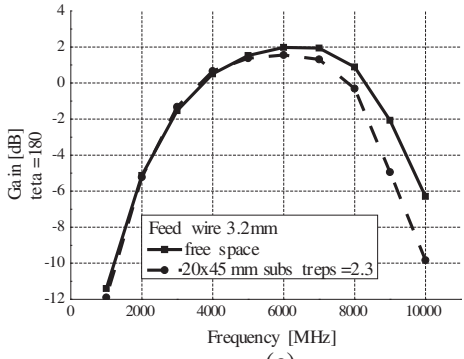

(c)

Figure 2. Elliptically-shaped dipole antenna with loop feeding (a), it's radiation pattern (b) and the antenna gain (c).

to the sampling unit by a 5 meter RF cable. The sampling unit is connected to the Digital Sampling Converter by custom data cables, the digitized signal is then transferred to the PC running the data acquisition software (Marcha) using the LPT port.

To excite the transmit antenna we used the 220 ps Gaussian-like pulse, which waveform and spectrum are shown in Figure 3.

The signal transmitted through the antenna pair by Tx-Rx antennas separation of 3 m is used as a reference signal. Its waveform and spectrum are shown in Figure 4.

3. NEAR-FIELD WIRELESS TRANSMISSION

Not much information can be found in literature on the near-field structure for different types of antennas. The most detailed investigation on the antenna near-field was done for an elementary electrical antenna [10]. In the vicinity of the antenna the electric

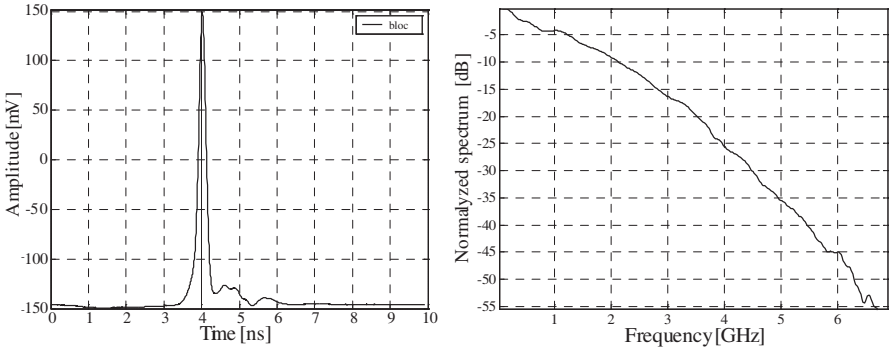

Figure 3. Pulse generator output waveform and spectrum.

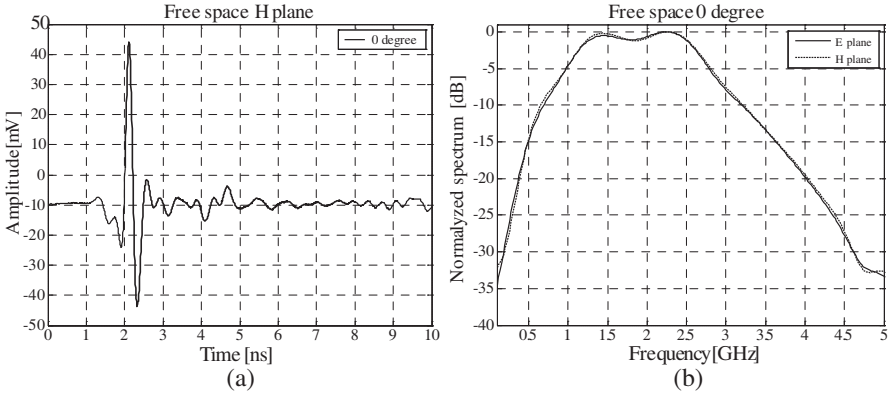

Figure 4. Received signal waveform (a) and its normalized spectrum (b). Antenna in a free space on a 3 m distance.

field does not only have a component $1/r$ dependence (where r is the distance to the radiation center of the antenna), but also components $1/r^2$ dependence and $1/r^3$ dependence. These components result in different from $1/r$ increase of field amplitude by approaching the radiation center of the antenna. It is reasonable to assume that such situation is typical for all electrically small antennas, since their field can be represented as a superposition of fields excited by a small number of such elementary antennas. Wheeler defined an electrically small antenna as one whose maximum dimension is less than $\lambda/2$ [11]. This relation is often expressed as: $ka < 1$ where $k = 2\pi/\lambda$ (radians/meter), λ is free space wavelength (in meters), and a is radius of sphere enclosing the maximum dimension of the antenna (in meters).

In 1959 Wheeler [12] also introduced a "radian sphere", where the reactive and radiation field components are equal in magnitude. From the practical side, the reactive near-field is often defined as the area within from the antenna aperture. Outside this distance reactive fields are negligibly small. What occurs between Wheelers "radian sphere" and the sphere has not yet been fully investigated.

3.1. Planar Elliptically Shaped Antenna Near-field

The goal of this sub-Section is to investigate the near-field distribution around an electrically small UWB antenna which will be used for the antenna on body scenario. Based on Wheeler's definition, the radius of the radian sphere for this antenna should be approximately between 0.5 cm and 1.6 cm (Table 1). In our case this area will be around the feeding point and will be smaller than the antenna. In order to describe the antenna near-field, we analyze the spatial distribution of the electromagnetic field within the 3λ sphere. In this investigation, we compute the electrical field distribution at different distances (from 0.1 mm to 35 cm) from the antenna along Z-axis, which is perpendicular to the antenna plane.

The computational model includes an antenna on a substrate with specified observation points at different distances from 0.1 mm to 35 cm. The theoretical antenna model has been described in [13].

Table 1. Calculation of the "radian sphere" radius R_W for the lowest and highest frequencies of the operational bandwidth.

Frequency	[GHz]	3	10
λ	[cm]	10	3
R_W	[cm]	1.6	0.47

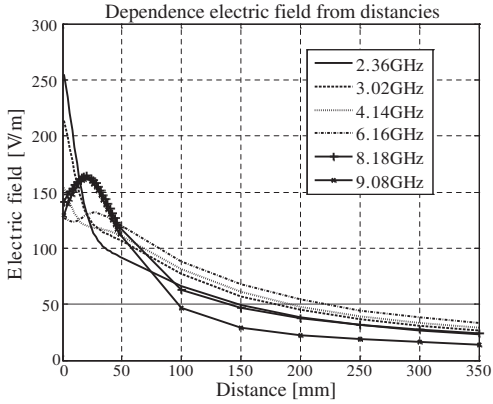

Figure 5. Dependence of the electric field on distance for different frequencies.

Simulation results for the tangential component of the electric field along main axis of antenna at different frequencies are presented in Figure 5. It can be seen that near the antenna the field distribution for different frequencies is different: while at low frequency the field strength increases by approaching the feed point, at higher frequencies a decrease of the field strength is observed.

A comparison of the antenna near-field distribution at the lowest and highest frequencies in the band with $1/r$ dependency is presented in Figure 6. At 2.34 GHz the deviation from the $1/r$-dependence occurs at distances smaller than 85 mm from the feed point; at the distance of about 27 mm the curve behavior changes again. At 9.08 GHz the deviation from $1/r$-dependence starts again at about 90 mm distance and from the distance of around 20 mm the field strength even decreases when approaching the feed point.

The obtained results show that components with dependences $1/r^2$ and $1/r^3$ do not result in an additional increase of the tangential field strength by approaching the feed point, but instead reduce the increase of the $1/r$ dependence. This can be explained physically that the radiation from the antenna occurs not only from the feed point, but also from both flairs. At short distances from the antenna, the interference of the fields radiated by elementary currents distributed over the antenna flairs leads to destructive behavior. The actual field strength considerably deviates from the $1/r$ distribution within the radian sphere of Wheeler. Outside of the Wheeler sphere a good agreement with the $1/r$ dependence is observed.

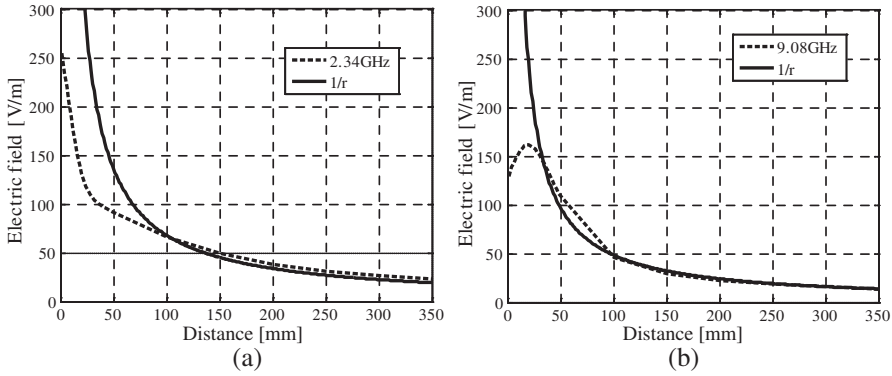

Figure 6. Tangential component of electric field versus the distance from the antenna feed point at 2.34 GHz (a) and 9.08 GHz (b).

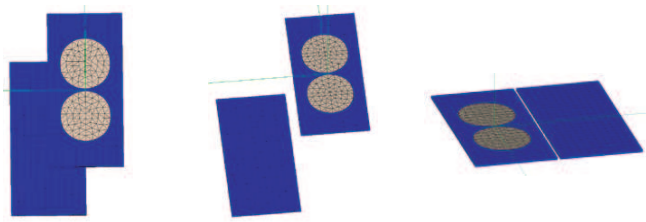

Figure 7. Different antenna locations: (a) end fire, (b) staggered, (c) collinear.

3.2. Pulse Transmission Through an Antenna Pair

Our next step is the investigation of pulse transmission through a transmit-receive antenna pair when one antenna is situated in the near-field of the other. We varied the distance between the antennas from 2 mm to 10 cm. We selected this range of distances as over this range the electric field strength distribution deviates from the $1/r$ dependence. At distances larger than 10 cm, the power budget of the transmission follows a well-established far-field behavior. We considered three scenarios in our investigation (Figure 7). In the first scenario both antennas are in the end-fire configuration (located face to face) (we counting out the distance between antenna feed points); in the second scenario the antennas are staggered (the antennas are separated in boresight direction by 10 mm and as the distance between antennas is counted as a shift in the antenna plane), but still stay

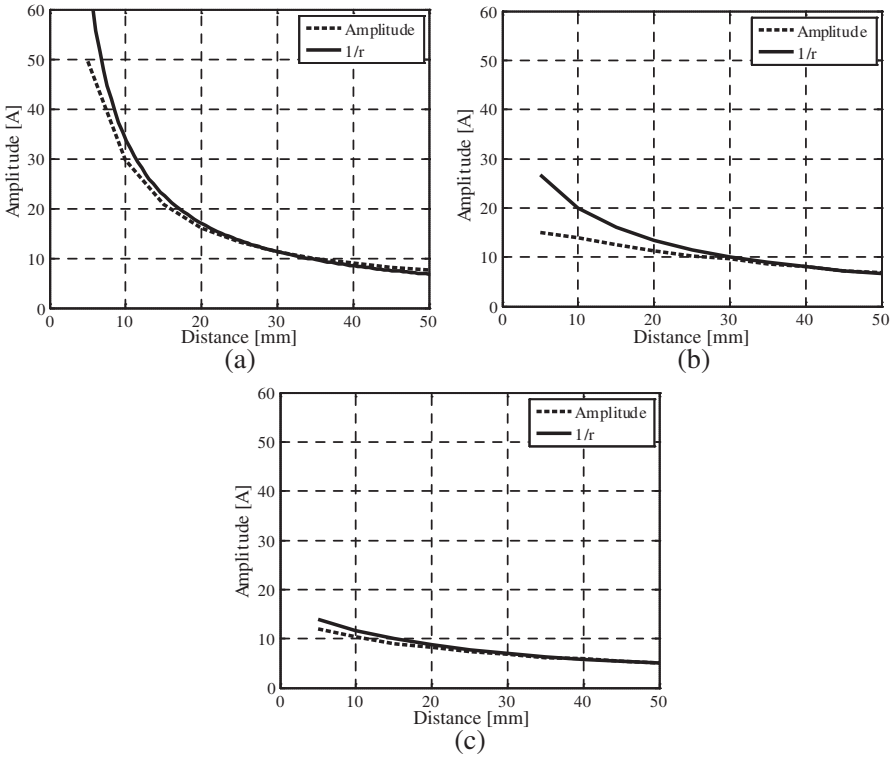

Figure 8. Pulse amplitude versus distances: (a) end fire (reference point is the antenna feed point), (b) staggered (reference point is the antenna flair), (c) collinear (reference point is the antenna flair).

face to face; and in the third scenario the antennas are collinear (the distance between antennas is counted as the distance between antenna substrates).

For investigation of the pulse transmission we use a Gaussian pulse with duration of about 200 ps. During the analysis we noted presence of the antenna coupling, which results in a decrease of the feed voltage at the transmit antenna of about 3%. This results in a corresponding decrease of the voltage at the receive antenna terminals.

We observe (Figure 8) that for the end-fire antenna configuration, the total power loss (in comparison with $1/r$ propagation model) might be as high as 3 dB at the antenna separation of 5 mm. At the same time for the staggered antenna configuration at the same distance the total power loss might be 11 dB and for the collinear configuration the power loss is roughly 12 dB.

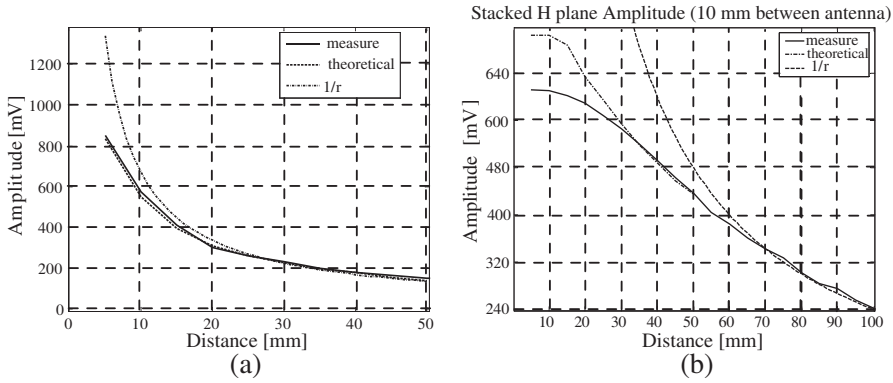

Figure 9. Antenna near field measurements: line-of-sight scenario (a) and stacked antenna scenario (b).

To confirm the theoretical results we performed near field measurements of the planar elliptically-shaped dipole antenna.

The antenna measurements vs. theoretical results are presented in Figure 9. For a line-of-sight scenario the theoretical and measured results are similar. However, for the staggered antenna scenario the theoretical and experimental results disagree at distances from 2 cm to 4 cm. Any shift from their initial position leads to a shift and overlapping of both antenna flairs with antenna feeding points. Due to such antenna overlapping, the theoretical model will experience more coupling between the antennas leading to the increase of the measured signal amplitude.

4. CONCLUSIONS

In this paper we have investigated UWB Impulse Radio transmission for different typical WPAN scenarios. We first theoretically investigated properties of the near field for small antenna of electrical type. Then we have studied theoretically and experimentally short-range UWB wireless link (wireless fire-wire).

We found that the antenna near-field distribution does not follow the $1/r$ model within a Wheeler sphere with an origin at the antenna feed point. The simulation results show that the strength of the tangential component of the electric field increases slower than a $1/r$ dependence by approaching the feed point. The distance, at which the actual field strength starts to deviate considerably from the $1/r$ distribution, is accurately predicted by the radian sphere of Wheeler.

The theoretical and experimental results on short-range transmission through a pair of UWB antennas demonstrate a deficit in power budget of a wireless link with two such antennas in comparison with a prediction based on far-field behavior only. The total power budget deficit for the scenario "end-fire" is of about 3 dB for an antenna separation of about 5 mm, while for other scenarios (staggered and collinear) the deficit can be as high as 15 dB.

Finally, we also demonstrated that near-field antenna coupling results in a decrease of the transmit antenna feeding voltage up to 3%.

REFERENCES

1. Win, M. Z. and R. A. Scholtz, "Impulse radio: How it works," *IEEE Communications Letters*, Vol. 2, No. 2, 36–38, Feb. 1998.
2. Klemm, M. and G. Tröster, "Small patch antennas for UWB wireless body area network," Electronics Laboratory, Swiss Federal Institute of Technology Zurich (ETH Zurich), 2007.
3. Nielsen, J. O. and G. F. Pedersen, "In-network evaluation of body-carried mobile terminal performance," *Proc. 12th IEEE International Symposium on Personal, Indoor and Mobile Radio Communications*, Vol. 1, D-109–D-113, Sep. 2001.
4. Nielsen, J. O., G. F. Pedersen, K. Olesen, and I. Z. Kovacs, "Statistic of measured body loss for mobile phones," *IEEE Transaction on Antennas and Propagation*, Vol. 49, No. 9, 1351–1353, Sep. 2001.
5. Kotterman, W. A. Th., G. F. Pedersen, K. Olesen, and P. Eggers, "Cable-less measurement set up for wireless handheld terminals," *Proc. 12th International Symposium On Personal in Door and Mobile Radio Communication (PIMRC)*, Vol. 1, B.112–B.116, Sep. 2001.
6. Alomainy, A., Y. Hao, C. G. Parini, and P. S. Hall, "Comparison between two different antennas for UWB on-body propagation measurements," *Antennas and Wireless Propagation Letters*, Vol. 4, 31–34, 2005.
7. Welch, T. B., R. L. Musselman, B. A. Emessiene, P. D. Gift, D. K. Choudhury, D. N. Cassadine, and S. M. Yano, "The effects of the human body on UWB signal propagation in an indoor environment," *IEEE Journal on Selected Areas in Communications*, Vol. 20, No. 9, 1778–1782, Dec. 2002.
8. Yarovoy, A. G. and A. V. Vorobyov, "Widening of operational frequency band of the loop antenna," *IEEE International*

Conference on Ultra-Wideband, 206–209, Zurich, Switzerland, 2005.

9. Bagga, S., A. V. Vorobyov, S. A. P. Haddad, A. G. Yarovoy, W. A. Serdijn, and J. R. Long, "Codesign of an impulse generator and miniaturized antennas for IR-UWB," *IEEE Transactions on Microwave Theory and Techniques*, Vol. 54, No. 4, 1656–1666, Apr. 2006.
10. Nikolskij, V. V., *Electrodynamics and Waves Propagation*, Moscow, Science, 1973 (in Russian).
11. Wheeler, H. A., "Fundamental limitation of small antennas," *Proceeding of the IRE*, Vol. 35, 1479–1484, 1947.
12. Wheeler, H. A., "The radiansphere around a small antenna," *Proceeding of the IRE*, Vol. 47, 1325–1331, 1959.
13. Vorobyov, A. V., A. G. Yarovoy, and L. P. Ligthart, "Influence of dielectric substrate size on UWB antenna performance," *Antem'05 Conference*, 140–141, San Malo, France, 2005.
14. Inanlou, F. and M. Ghovanloo, "Wideband near-field data transmission using pulse harmonic modulation," *IEEE Transactions on Circuits and Systems I: Regular Papers*, Vol. 58, No. 1, 186–195, 2011.
15. Yin, W. Y., G. H. Nan, and I. Wolff, "The near and far field distributions of a thin circular loop antenna in a radially multilayered biisotropic sphere," *Progress In Electromagnetics Research*, Vol. 21, 103–135, 1999.
16. Liu, X.-F., B.-Z. Wang, S.-Q. Xiao, and J. H. Deng, "Performance of impulse radio UWB communications based on time reversal technique," *Progress In Electromagnetics Research*, Vol. 79, 401–413, 2008.